VELOCITY AND DROP SIZE DISTRIBUTIONS DOWNSTREAM GENERIC CLUTTER ELEMENTS FOUND WITHIN ENGINE NACELLES†

Peter J. Disimile and James R. Tucker
USAF 46 Test Wing, Aerospace Survivability and Safety Flight
2700 D Street, Bldg 1661
Wright-Patterson AFB, Ohio 45433-7605, USA
peter.disimile@wpafb.af.mil
937-255-6823 ext. 212

Joe Stern, Luke Mehl, and Brian Croswell
UC-FEST, Department of Aerospace Engineering, University of Cincinnati
Cincinnati, Ohio 45221-0070, USA

ABSTRACT

The current work is presented as part of an effort to help develop a spray transport model that would be used within the computational fire code currently under development by Sandia National Laboratory. As part of a halon replacement research program, new high-boiling-point chemical suppressants have been identified. These agents would discharge in a liquid state, breaking into liquid droplets, and be entrained within the flow passing through the nacelle, impinging on various objects prior to reaching the fire zone. The goal of this research effort is to enhance the fundamental knowledge of spray interactions with clutter (e.g., obstacles representing fuel and hydraulic lines, electrical wire bundles, etc). Three-dimensional velocity and diameter data was collected at two locations downstream for nine combinations of clutter spacing and coflow airspeed. Analysis of velocity and diameter data consisted of polynomial regression and trigonometric analysis, which enabled the construction of mathematical correlations for the data.

INTRODUCTION

Aircraft engine nacelles represent a unique environment for fires and fire protection. Many nacelles are characterized by high air exchange rates and a strong degree of nonuniformity and turbulence within the airflow[(1)]. In addition, nacelles contain large amounts of plumbing, wiring, avionics and mechanical components mounted on the engine or along the nacelle walls. Some nacelles also contain large structural ribs. This combination of a highly turbulent airflow, flammable fluids, and numerous ignition sources makes aircraft engine nacelles a difficult fire zone to protect.

For the past several decades, halogenated agents, notably Halon 1301, have protected engine nacelles. Since the production ban on halon, scientists and engineers in the public and private sectors have been working on replacement agents and new technologies that attempt to replicate Halon 1301's beneficial attributes. Thus far, no one has succeeded completely. Of the technologies that have been deemed acceptable, based on environmental friendliness, toxicity, materials compatibility, etc., all lack fire-suppression efficiency as measured by weight and/or volume[(2)].

To improve the fire-suppression efficiency of these candidate technologies, one area of focus is suppressant distribution. Since Halon 1301 was so efficient, research into understanding the engine nacelle airflow offered little advantage. Today, however, a better understanding of the nacelle airflow and how it influences the spread of fires and fire extinguishing agents can have a large impact on the effectiveness of a halon replacement system.

An additional complication is due to the fact that some halon replacements are high-boiling point fluids when compared to Halon 1301. These can prove to be especially challenging to distribute in an aircraft engine nacelle. To understand how these systems would perform and thereby optimize a design, engineers must better understand how a spray of liquid droplets behaves when moving within a highly turbulent airflow found in cluttered engine nacelles. To this end, the present program focuses on the ability of water sprays to pass through a series of cylindrical obstacles, representing generic clutter, while moving in a turbulent coflow. A previous paper[3] examined the volume of suppressant that could pass through the current clutter packages and reach a potential downstream fire zone. Results indicated that the amount of suppressant captured by the clutter was directly related to the streamwise spacing of the clutter and coflow air speed at the clutter location. The current paper extends these results, documenting the velocity and drop size distribution both upstream and downstream of the clutter.

Nomenclature

D	clutter element diameter [mm]
DD	distance downstream from clutter package [measured in terms of the clutter element diameter]
CS	streamwise distance between clutter element arrays [measured in terms of the clutter element diameter]
X	downstream distance from the turbulence generator [mm]
Y	vertical distance from test section centerline [mm]
Z	transverse distance along clutter elements along centerline [mm]
U	streamwise droplet velocity [m/s]
V	droplet velocity in the transverse direction [m/s]
W	droplet velocity in the horizontal or lateral plane [m/s]
D_{32}	Sauter mean diameter of droplet [μm]
U_c	nominal streamwise coflow airspeed [m/s]

Suppressant Spray Flow Facility (SF)[2]

A low-speed flow facility with the test section air speed ranging from 0.0 to 12.0 m/s (0.0 to 39.4 ft/s) was modified for the current program. The major components of this facility include an inlet contraction, turbulence generator, test section, clutter section, and the return and separation plenum. A general overview of these components is provided in the following text.

Air drawn from a large laboratory is accelerated towards the test section through a 3.5:1 inlet contraction. This airflow is referred to as the test section coflow. To minimize outside disturbances from propagating directly into the test section, a flow-conditioning unit was

positioned at the contraction of the inlet. Immediately downstream of the inlet contraction, the coflow passes through a turbulence generation section and farther into the test section. The test section was divided into two zones, one upstream (zone A) and one downstream (zone B). The upstream portion of the test section (zone A) is shown in Figure 1.

Zone A contains the dual fluid suppressant spray nozzle and the clutter package. Zone B represents the remaining portion of the test section located downstream of the clutter package. Both zones have a 609.60 ± 0.79 mm x 914.40 ± 0.79 mm (24.00" ± 0.03" x 36.00" ± 0.03") cross sectional area. Zone A is 1219.00 ± 0.79 mm (48.00" ± 0.03") in streamwise length, while zone B is 2438.40 ± 0.79 mm (96.00" ± 0.03") in streamwise length. As previously noted, provisions have been made for the insertion of clutter packages at the downstream end of zone A. The leading edge of the clutter package is held fixed at 952.50 ± 0.79 mm (37.50" ± 0.03") downstream of the turbulence generation grid. The exit of the suppressant spray nozzle is located within the coflow, 596.90 ± 0.79 mm (23.50" ± 0.03") downstream of the turbulence generation grid; the nozzle exit is positioned along the coflow centerline, located 304.80 ± 0.79 mm (12.00" ± 0.03") vertically and 457.20 ± 0.79 mm (18.00" ± 0.03") horizontally from the test section walls. This also corresponds to the nozzle exit being located 355.60 ± 0.79 mm (14.00" ± 0.03") or 7 clutter diameters, D, upstream of the leading edge of the clutter package.

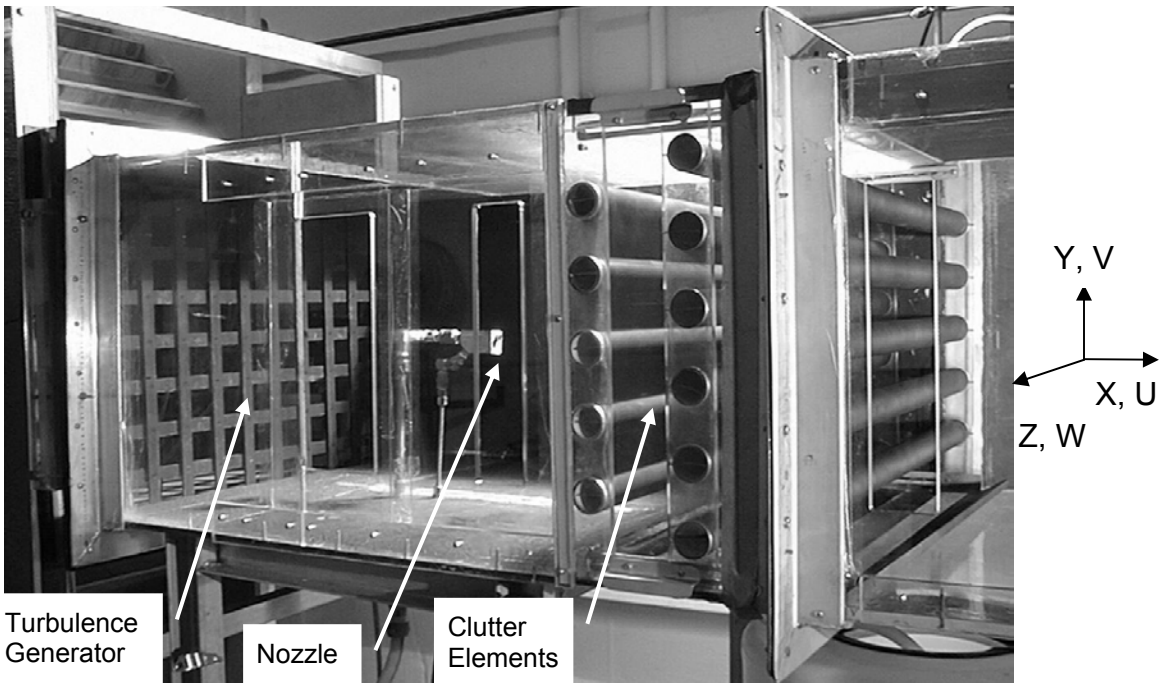

Figure 1: $(SF)^2$ Zone A Test Section

Turbulence Generator

A large grid consisting of several 25.40 ± 0.79 mm (1.00 ± 0.03 inches) wide, 6.35 ± 0.79 mm (0.25 ± 0.03 inches) thick, sharp-edged flat steel slats, spanning the cross-sectional area of the test section, were assembled in a checkerboard pattern with open cell dimension between the slats of 50.80 ± 0.79 mm x 50.80 ± 0.79 mm (2.00 ± 0.03 inches x 2.00 ± 0.03 inches). This grid

is also visible in Figure 1. Velocity surveys using constant temperature anemometry were acquired downstream of the turbulence generator, at x = 711.20 ± 0.79 mm (28.00 ± 0.03 inches). A wave-like distribution of the streamwise component of the mean velocity was observed with velocities ranging from approximately 3.7 m/s to 5.0 m/s (12.1 ft/s to 16.4 ft/s). Although general symmetry can be observed it appears that the lower portion of the test section seemed to have a greater degree of unsteadiness. It is believed that additional unsteadiness was a result of smoke generation supply tubes positioned at the entrance of the inlet contraction. In a similar manner turbulent intensities were recorded and ranged between 10 and 14%.

Clutter Package

The clutter package used in the current test series can be seen installed within zone A of the $(SF)^2$ test section (Figure 1). The present clutter package consists of 16 two-dimensional elements, spanning the width of the test section. These elements were cylindrical segments made from sections of PVC plastic tubing. Elements were assembled to form three separate arrays with equally spaced rows of 5, 6, and 5 tube elements, separated vertically by 47.75 ± 0.79 mm (1.69 ± 0.03 inches) or 0.94D between each cylindrical element. The elements have an outer diameter of 50.80 ± 0.79 mm (2.00 ± 0.03 inches). The streamwise spacing between each clutter array is variable, ranging from 12.70 mm (0.50 inches) to 101.60 mm (4.00 inches) with an error of 3.18 mm (0.13 inches). In terms of element diameter, the spacing ranges from 0.25 D to 2.00 D with an error of ± 0.06 D (Figure 2).

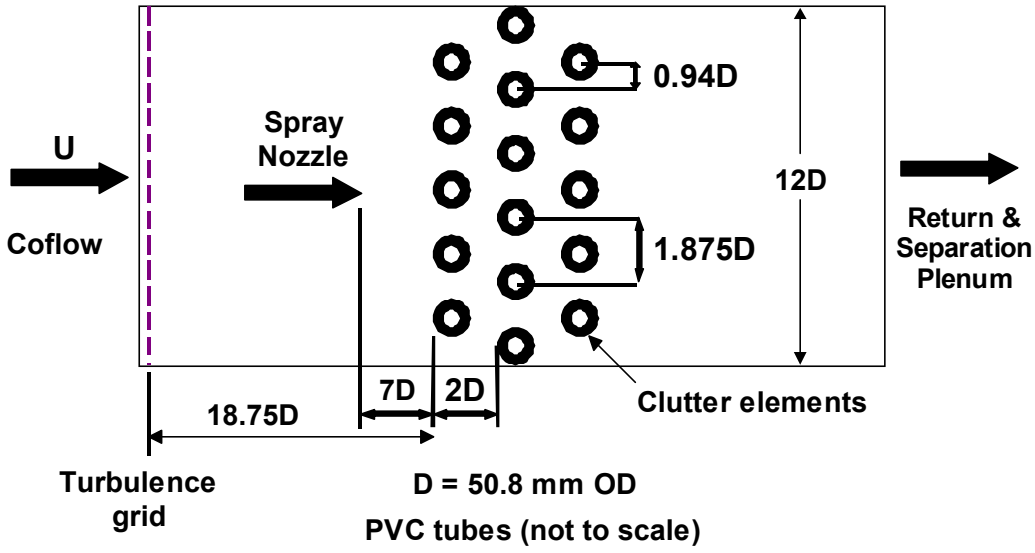

Figure 2: Side View Schematic of SF^2 Test Section

Phase Doppler Anemometry System

A three-dimensional Phase Doppler Anemometer (PDA) was used to simultaneously acquire velocity components and the diameter of the liquid drops exiting the suppressant spray nozzle. To position the PDA measuring volume in the center of the test section, 1000 mm lenses were

used on both the transmitting and receiving optics. Based on a previous study by Davis and Disimile[4], this measurement configuration also utilized the largest spatial filter (Mask A) in the receiving optics. In this configuration the maximum drop diameter capable of being measured was 810.8 μm.

Experimental Strategy

Air drawn through a two-dimensional contraction is conditioned and passed through a turbulence generator section, producing a 10% turbulent intensity (T.I.) level. This air stream enters the $(SF)^2$ test section and serves as a coflow for agent discharge. Agent discharge is generated using a dual fluid nozzle located on the centerline of the test section and directed downstream toward the clutter elements; however, the nozzle was slightly misaligned off-center, providing bias in the -y and +z directions. Water and air are mixed by the dual fluid nozzle and travel toward the leading edge of the clutter package. The suppressant droplets not captured by the clutter package proceeded downstream, where their three-dimensional velocity and diameters were measured using the Phase Doppler Anemometry (PDA) system. The measurement volume of the PDA system was located at 2.0 and 5.5 clutter diameters downstream of the trailing edge of the final clutter array. The measurement volume was traversed along the vertical axis from 140.00 ± 0.79 mm (5.51 ± 0.03 inches) above to 140.00 ± 0.79 mm below the horizontal centerline at each downstream measurement location.

General Strategy

The spray nozzle water flow rate was set and maintained at 17.1 ± 0.4 L/min (4.5 ± 0.1 gal/min) with a corresponding nozzle water pressure of 158.0 ± 13.7 kPa (23.0 ± 2.0 psi). The water flow was monitored using a turbine type flowmeter positioned directly upstream of a pressure gage. The incoming air was regulated to a pressure of 171.8 ± 3.4 kPa (25.0 ± 0.5 psi). The test matrix consisted of 18 experimental conditions. This included three coflow speeds, three clutter densities, and two downstream measurement locations. Clutter package densities were varied by changes in the streamwise spacing between individual clutter arrays. Array spacing was selected to be 0.25 D, 1.00 D, and 2.00 D with an error of ± 0.06 D. In the current study D = 50.80 ± 0.79 mm (2.00 ± 0.03 inches). Since the leading edge of the clutter package was fixed, changing the array spacing affected the location of the trailing edge of the last clutter element. Therefore, to maintain a fixed downstream location of the PDA measurement volume with respect to the trailing edge of the clutter, the PDA measurement volume had to be moved correspondingly with the trailing edge movement.

Previous experiments were conducted to determine the volume of water transmitted through the clutter package as a function of the streamwise spacing of the clutter array and coflow speed. During these experiments, a repeatable procedure for measuring the liquid water volume was followed and previously reported[3]. Based on these studies, air speeds of 3.0 m/s, 4.0 m/s, and 5.0 m/s were chosen for the current investigation.

PDA Strategy

Initial PDA measurements[3] acquired upstream of the clutter package included velocity and diameter traverses. These were performed at the center of the zone A test section (z = 0) at a location 2D (101.60 ± 0.79 mm or 4.00 ± 0.03 inches) upstream from the leading edge of the clutter package. Specifically, 20,000 data points were acquired at 37 positions through the center of the air/water spray. Each vertical position was spatially separated by 3.155 ± 0.022 mm (0.124 inches ± 0.001 inches). The center of the spray nozzle was identified as the location where the streamwise component of the mean velocity, U, reached a maximum while the lowest Sauter and arithmetic mean diameters were observed. The coflow air speed was maintained at a constant value of 5.00 m/s ± 0.25(5%) m/s (16.40 ft/s ± 0.82 ft/s) during PDA acquisition. A typical streamwise velocity vector and arithmetic mean plot is shown in Figure 3; the inverse

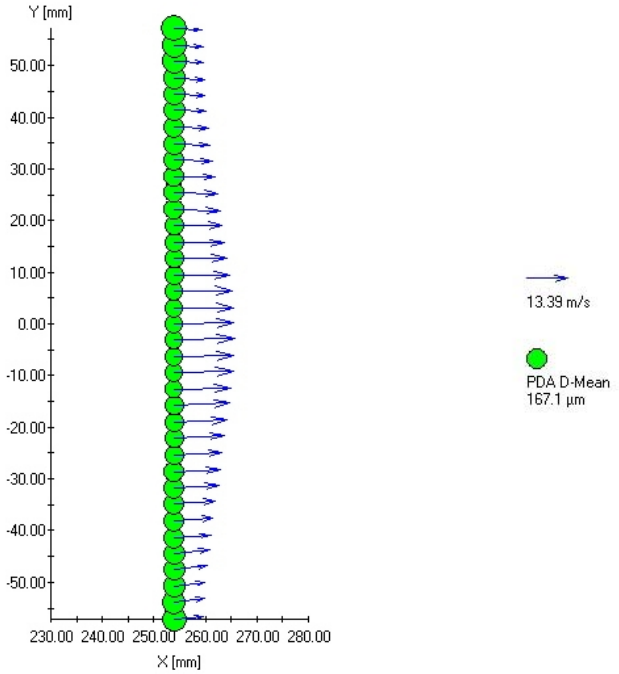

Figure 3: UV Vector and Arithmetic Mean Diameter Plot

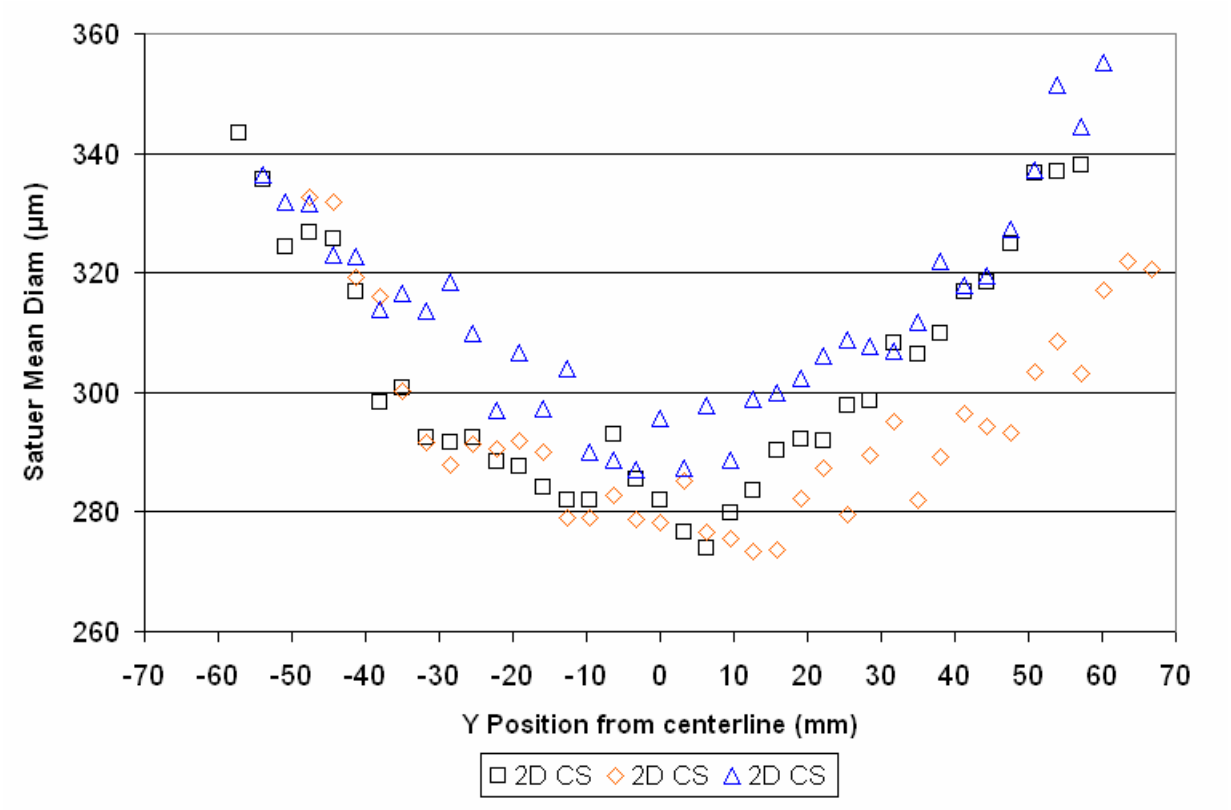

Figure 4: Sauter Mean Diameter Profiles 2.0 D Upstream of Clutter (5.0 m/s)

relationship between droplet velocity and diameter upstream of the clutter array can also be seen downstream of the array. A Sauter diameter plot collected upstream of the clutter is shown in Figure 4. Droplet data was collected downstream of the trailing edge of the clutter package at downstream locations of 2.0 and 5.5 DD using the same PDA strategy as upstream data acquisition.

Data Analysis Strategy

The downstream 3-D velocity and diameter data were imported, plotted, and analyzed in Excel. Each data component (U, V, W, and D_{32}) was grouped by each independent parameter: clutter spacing, downstream distance, and coflow speed.

Overall, the most appropriate polynomial regression of the data was of degree six. Thus, five observable changes in direction of the data were noticed; however, since this was the limit of Excel's built-in capabilities, no higher-order polynomial regression could be examined.

The final organization of data resulted in variation of coflow speed at constant downstream distance and clutter spacing. This revealed similarities in each flow, and a parabolic fit was placed on each of the three segments of data, as defined by the periodic pattern of high and low peaks in both velocity and diameter data. Since a sixth-degree polynomial must be smooth and continuous across the entire domain, three separate parabolic fits allowed for discontinuities

where the data was neither smooth nor asymptotically stable—approaching a finite limit—from visual observation. These discontinuities in the data could be overcome by the parabolic approach. Each of the three parabolas for each test was manually fit to the data; rather than a regression, which would provide an average of values, the manual fit provided an upper bound to the data.

Resolving each of the six plots of U and V data at varying coflow speed, U_c, resulted in six groups of three parabolas; this data was then collapsed by taking the three parabolic coefficients a, b, and c at each U_c and creating a relation for each coefficient as a function of U_c. A second-degree polynomial regression was used for each coefficient at the three values for U_c, providing the functions $a(U_c)$, $b(U_c)$, and $c(U_c)$ for each parabolic fit, reducing all U data to three parabolic functions for each clutter spacing. The same procedure was conducted for the V data; however, neither W nor D provided enough of a pattern for such parabolic fits.

Once the periodic nature of the data was observed, an Excel-based fast Fourier transform (FFT) algorithm was used to construct trigonometric models of all data. This method was needed only to build a mathematical function relating the vertical position (Y) to U, V, W, or D_{32}. No regression (with the intention to further collapse the data) was provided from the FFT method.

Suppressant Transport Results and Discussion

Varying such parameters as coflow speed and clutter spacing produced varying results for U, V, W, and D_{32}. However, similarities between all related data sets (e.g. all U data at 2.0 D downstream) were noticed when these data sets were plotted together. For instance, the qualitative relationship of peaks in droplet velocity and diameter data along the vertical direction corresponded to the location of clutter elements in the vertical direction. Quantitatively, proportionality of the peaks to the element locations has not yet been established; however, the mathematical methods in use will continue to provide insight into these relationships. In Figures 5 through 10 below, all U, V, and D_{32} data at the 2.0 DD and 5.5 DD locations were plotted as a function of vertical position, Y. The vertical positions of each clutter element were also placed on each figure, along with a representation of the clutter elements along the vertical span of the traverse.

In Figures 5 through 7, all data recorded 2.0 DD of the trailing edge of the clutter is presented. At this location, a pattern common to all data can be noticed: the data behaves periodically in correlation to the vertical location of the clutter elements.

For the U data (Figure 5), the various data all show peaks in magnitude at the locations of the front/rear clutter elements and low points at the middle clutter elements. With the exception of the 1.0 m/s, 0.25 D CS case, every combination of horizontal spacing of clutter elements and nominal coflow speed examined shows this pattern. In all cases, the 0.25 D CS data showed the least conformity to the rest of the data at a given coflow speed, with the 5.0 m/s, 0.25 D CS data representing the upper extreme.

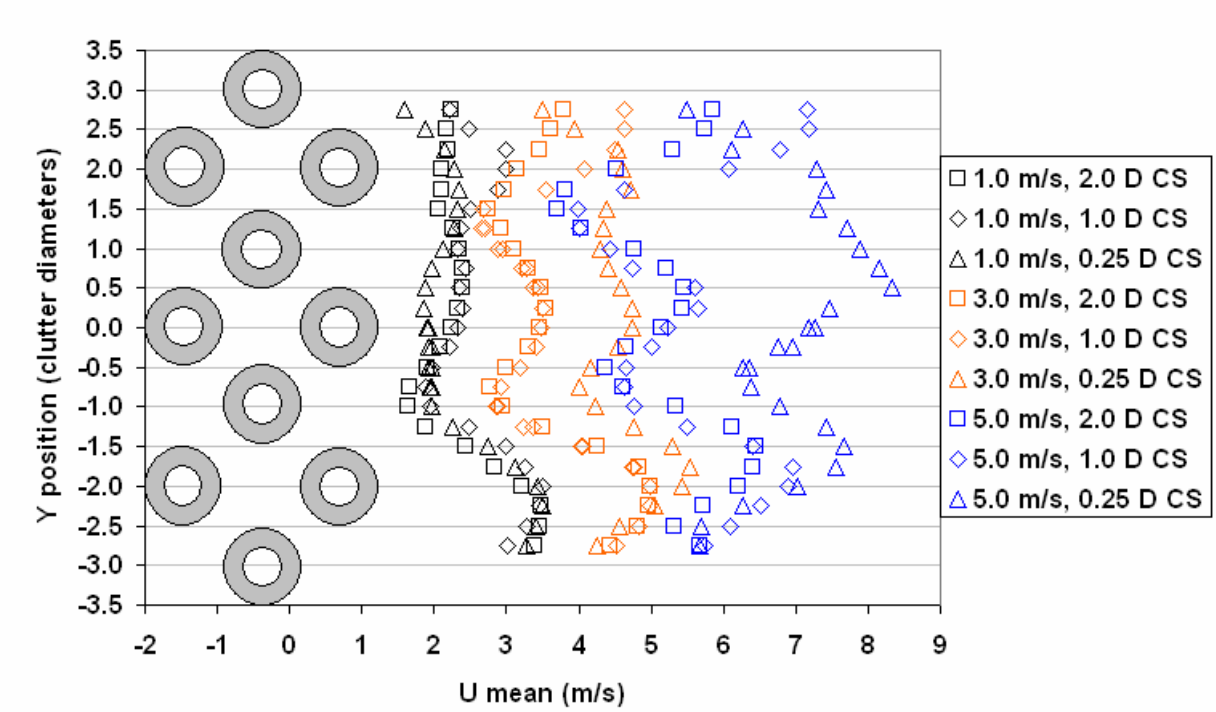

Figure 5: U Velocity Data at 2.0 D Downstream for Various U_C, CS

The V data (Figure 6) shows a similar trend to the U data: peaks in magnitude correspond to the front/rear clutter elements, while low points correspond to the middle elements. Notice that increasing U is plotted from left to right, whereas increasing V is plotted from right to left; taking this into account, the same trend observed in U (three peaks pointing toward 9 m/s) can be observed in V (three peaks pointing toward –5 m/s). Very few data points show that droplets carried any upward positive velocity at 2.0 D downstream. Again, the 0.25 D CS data (at 5.0 m/s and also 3.0 m/s U_C) showed noticeable deviation from the rest of the data. While U also increased toward the floor of the test section, the same observation of V is emphasized.

The Sauter diameter, D_{32} (weighted mean derived from volume divided by surface area), showed a similar periodic trend (Figure 7) inversely related to the velocity data. Whereas U and V data both showed peaks at the front/rear elements and low points at the middle, D_{32} showed low points at the top of the front/rear elements and peaks at the tops of the middle. Most droplet diameters were measured in the 200 to 400 µm range at 2.0 D downstream. The noticeable change between 2.0 and 5.5 D downstream is noted below. Since the nozzle was biased downward (as noted in Experimental Strategy), this correlation between the peaks in the U and V data and the peaks in the D_{32} data may be misleading in the figures above; however, the inverse relationship between velocity and diameter trends is supported by Figure 3.

Data at 5.5 DD was also analyzed (Figures 8 through 10). Upon initial inspection, the periodic pattern noted at 2.0 D downstream is no longer noticeable. The velocity profiles at this location have smoothed out to reveal a single peak in magnitude, occurring around the test section centerline. At 5.5 DD, the periodicity of the velocity data is reduced and symmetry along the vertical axis is increased.

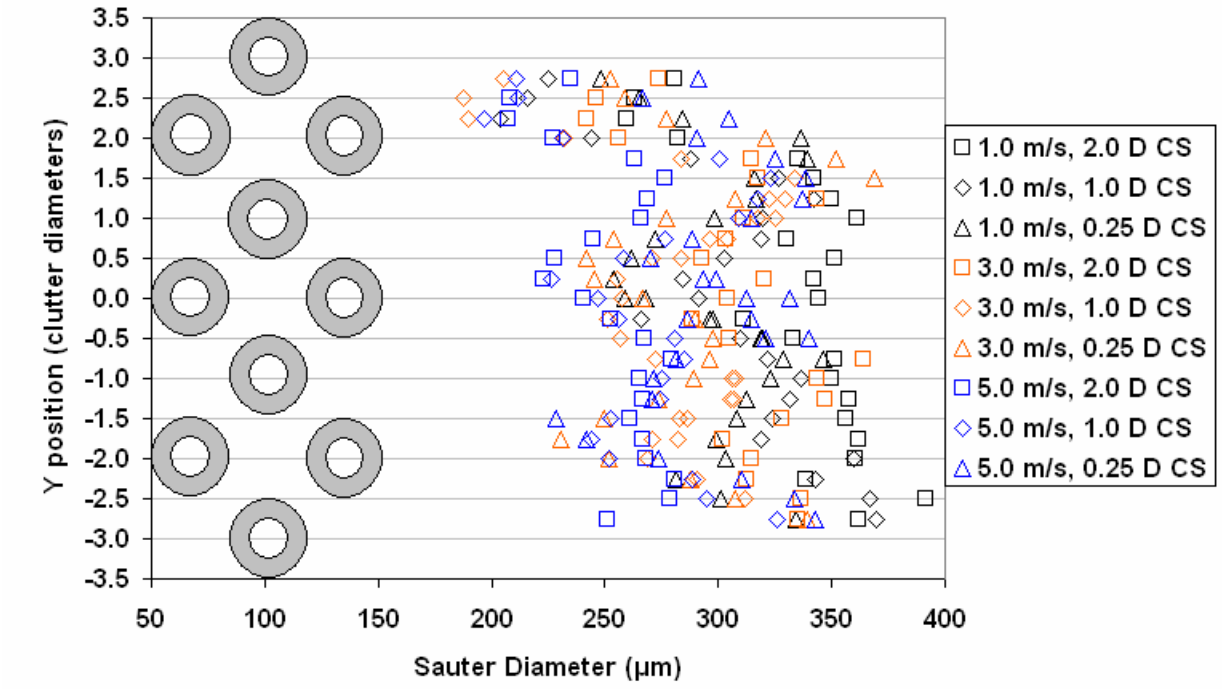

Figure 6: V Velocity Data at 2.0 D Downstream for Various U_C, CS

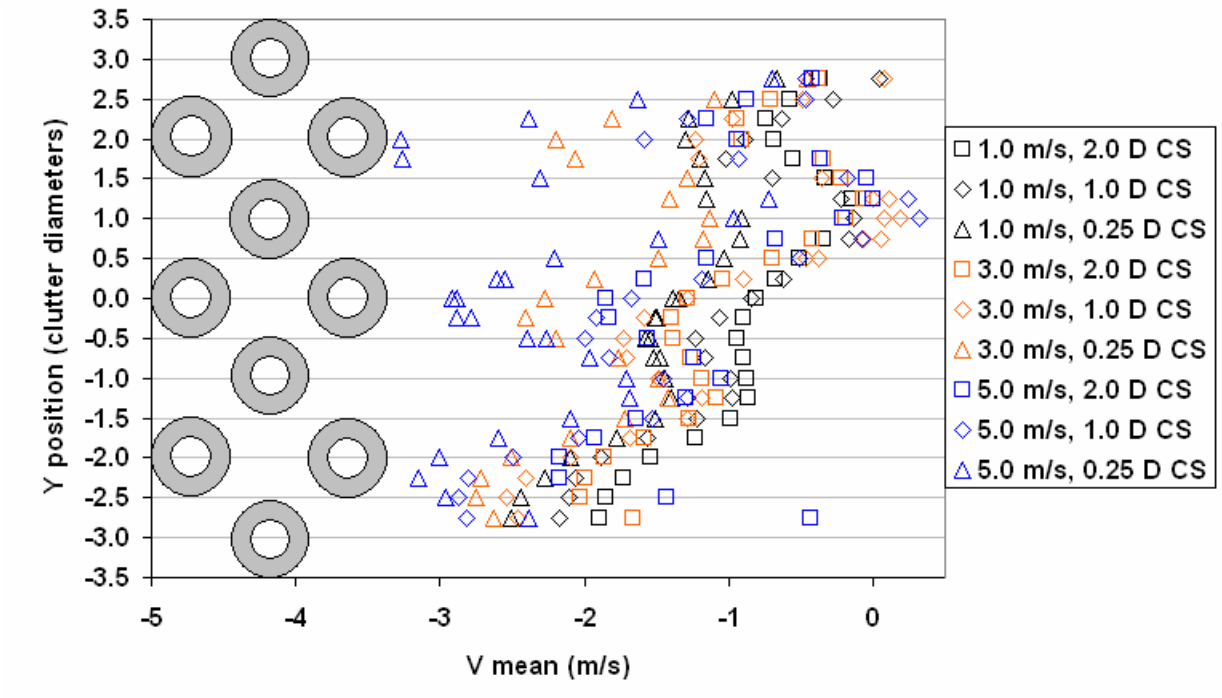

Figure 7: Sauter Diameter Data at 2.0 D Downstream for Various U_C, CS

In Figure 8, two trends in U data can be observed; the more common trend involves a slight decrease in velocity near the centerline. The less common trend involves (as Y progresses from +3.5 to –3.5 D) a rapid increase in velocity and then a slight decrease in velocity; this is seen in

the data at 0.25 D CS (at 1.0 and 3.0 m/s coflow speeds). Again, data at 0.25 D CS (for both 3.0 and 5.0 m/s U_C) follows similar trends to the rest of the data, but it is less pronounced. Besides deviating in velocity, data at these two configurations also deviate in the pattern; rather than decreasing near the centerline, these two data sets increase strongly. Even though other data sets at 5.0 m/s deviate from the rest of the data, they still follow the same trend.

The V data at 5.5 D downstream (Figure 9) showed double the number of data points at which droplets carried any upward velocity than did the data at 2.0 D downstream. Most of the data conformed to a trend of (from Y = +3.5 to –3.5 D) low negative velocity to increasingly negative velocity. The other trend is of very low velocity far from the centerline to very highly negative velocity near the centerline. The data to show this pattern are all at 0.25 D CS; the higher coflow speeds showed the greatest change in velocity along the vertical direction.

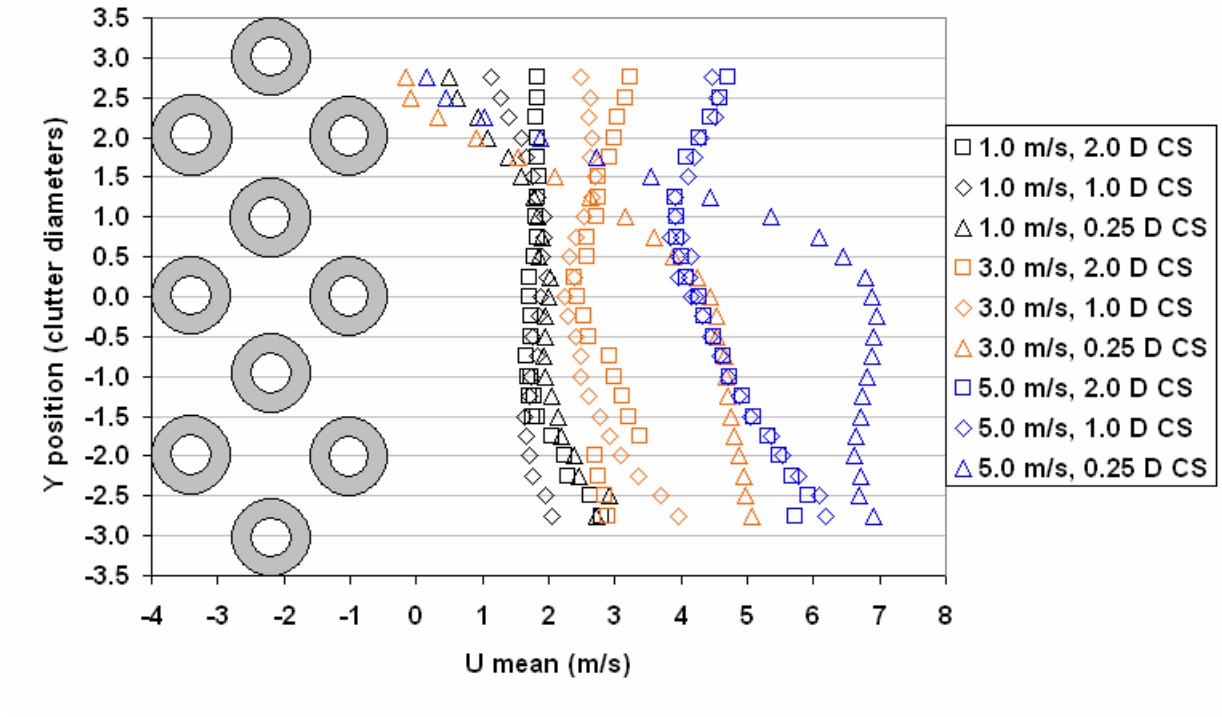

Figure 8: U Velocity Data at 5.5 D Downstream for Various U_C, CS

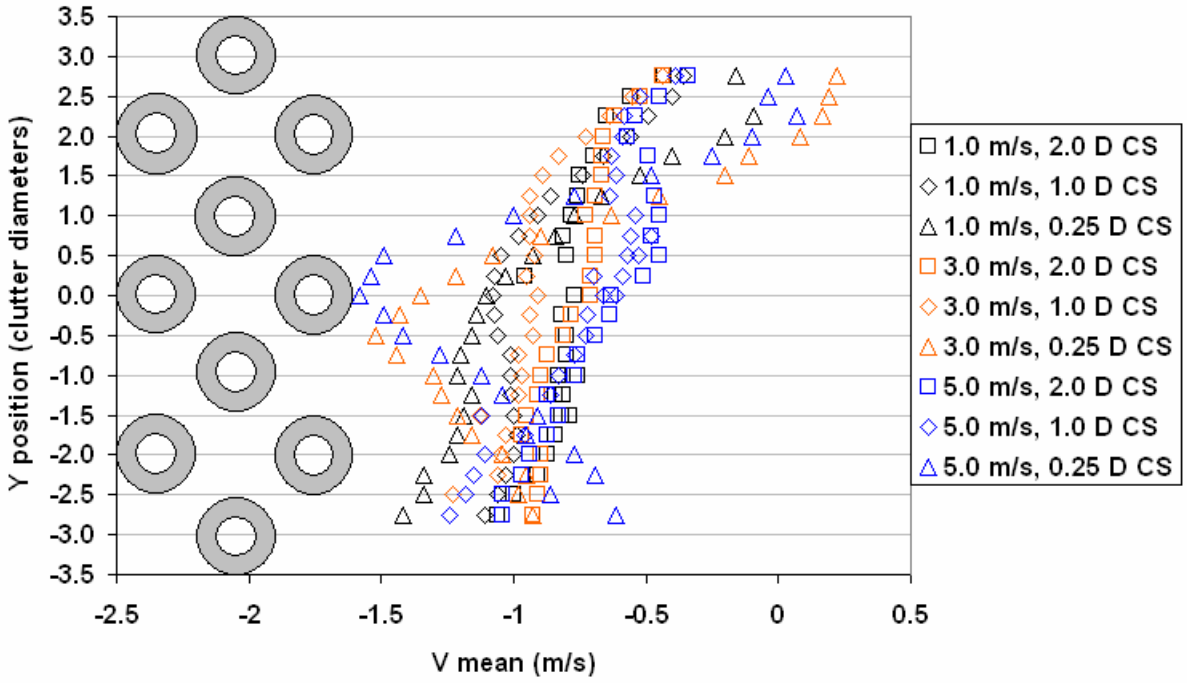

Figure 9: V Velocity Data at 5.5 D Downstream for Various U_C, CS

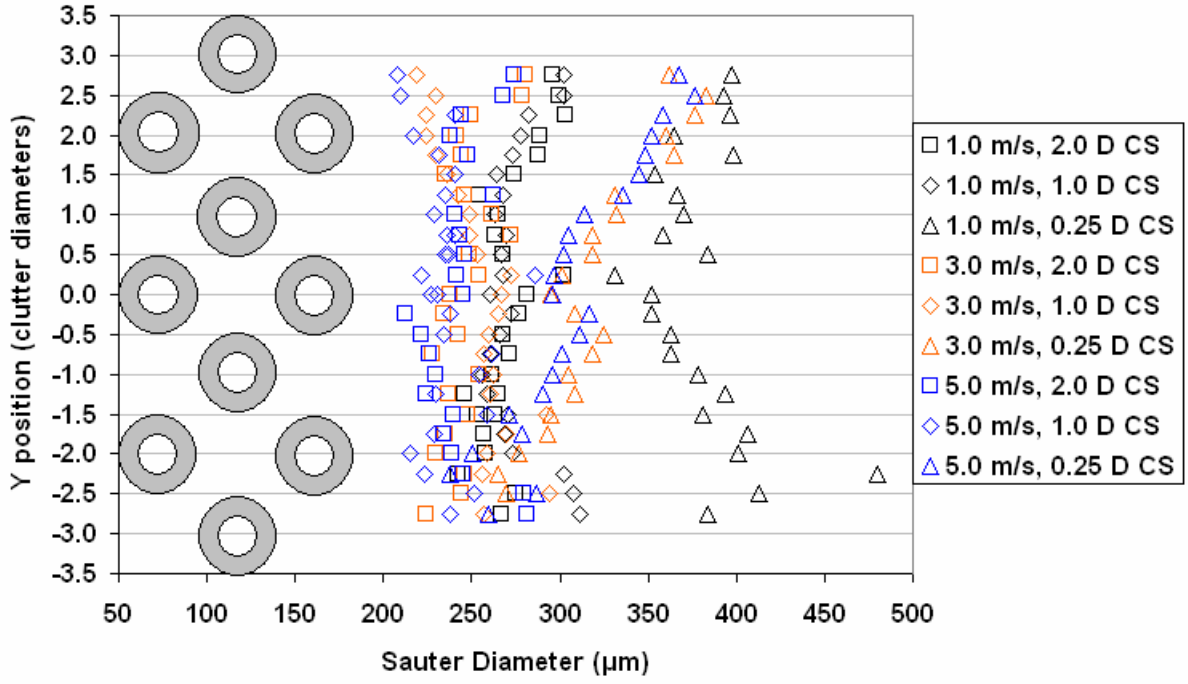

Figure 10: Sauter Diameter Data at 5.5 D Downstream for Various U_C, CS

The diameter data at 5.5 D downstream (Figure 10) shows consistency. Except for 0.25 D CS data, all other data showed relatively little change in diameter along the vertical direction. 2.0 D CS data decreases slightly in diameter as Y decreases, while 1.0 D CS data increases slightly. The range of mean diameters has changed since 2.0 D downstream; also, the concentration of Sauter diameters has decreased from approximately 300 μm at 2.0 DD to approximately 250 μm at 5.5 DD.

The data collected at 2.0 DD was analyzed using three methods (in the Data Analysis Strategy section); six-degree polynomials, multiple parabolas, and Fourier analyses were applied to the data in Figures 5 through 7. The main goal was to collapse the data to few formulas, rather than individual data points. Little physical significance was yet found in the coefficients for the analysis methods; however, velocity and diameter data series could be reproduced with these methods, including the periodic trends and peaks in the data. So far, the parabolic/regression method has provided the best results, while the Fourier analysis represented the data series more selectively.

Multiple data series have been collapsed into one set of formulas; for example, all of the U data at 1.0 D CS, for varying coflow speeds, can be represented by a set of formulas derived from the parabolic/regression method. In the future, models allowing clutter spacing and not only coflow speed will be developed. In short, one set of three parabolic equations has been developed for each clutter spacing. For example, at 1.0 DC (at 2.0 DD and between 3 and 4 m/s U_C), the set of three equations for U [m/s] (each equation representing a separate peak in the U data seen in Figure 5) as functions of U_C [m/s] and Y [mm] is shown below:

$$U = \begin{cases} \left(\frac{-.000130}{2}(U_C - 5) - 6.97\text{E}-4\right)Y^2 + \left(\frac{-.0104}{2}(U_C - 5) - 0.135\right)Y + 2.29(U_C - 5) + .446 \\ \left(\frac{-.000365}{2}(U_C - 5) - 6.31\text{E}-4\right)Y^2 + \left(\frac{.0149}{2}(U_C - 5) + 1.89\text{E}-2\right)Y + 2.02(U_C - 5) + 5.54 \\ \left(\frac{-.00040}{2}(U_C - 5) - 9.47\text{E}-4\right)Y^2 + \left(\frac{.108}{2}(U_C - 5) + 0.253\right)Y - 4.64(U_C - 5) - 9.65 \end{cases}$$

If physical significance cannot be identified in the coefficients of these formulas, then at least multiple sets of empirical data may be collapsed to very few formulas for development of Sandia's fire code.

Summary

In continuation of "The Transport of Water Sprays Past Generic Clutter Elements Found Within Engine Nacelles,"[3] flow field parameters such as downstream distance of the measurement volume, spacing between the clutter elements, and coflow airspeed were varied in order to advance the mathematical understanding of the flow field. Analysis of all collected data (U, V, W, and D_{32}) included both polynomial regression (primarily of U and V) and trigonometric regression (due to the periodic nature of all data). Periodic trends were observed in all data; at 2.0 D downstream, velocity and diameter data showed a trend of peaks in values corresponding

to front/rear clutter elements and low points corresponding to middle elements. At 5.5 D downstream, however, the periodic nature dissipated.

Acknowledgements

This research is in part supported by the Department of Defense's Next Generation Fire Suppression Technology Program, funded by the DoD Strategic Environmental Research and Development Program. The authors would like to thank Dr. Dave Keyser acting on behalf of Naval Air Systems Command for coordinating this activity as well as providing invaluable discussion relating to the experiments. We would also like to thank Mr. John Davis with the University of Cincinnati and Mr. Nathaniel McElroy with Veridian Engineering (now General Dynamics Advanced Engineering Information Systems) for their technical support.

References

[1] Black AR, Suo-Anttila JM, Disimile PJ, Tucker JR. Numerical predictions and experimental results of air flow in a smooth quarter-scale nacelle. AIAA Paper 2002-0856, Virginia, USA 2002, 16pp.

[2] Grosshandler W, Presser C, Lowe D, Rinkinen W. Assessing halon alternatives for aircraft engine nacelle fire suppression. ASME Transaction Journal of Heat Transfer 1995;117:2.

[3] Disimile PJ, Tucker JR, Croswell B, Davis J. The Transport of Water Sprays Past Generic Clutter Elements Found Within Engine Nacelles. Halon Options Technical Working Conference 2003.

[4] Davis JM, Disimile, PJ. "The Effect of Lens/Aperture Selection On Phase Doppler Anemometer Measurements", AIAA 2004-604, 42nd AIAA Aerospace Sciences Meeting and Exhibit, Reno, Nevada, 5-8 January 2004.